

## Temperature-dependent Al/GaAs(110) interface formation and adatom energy references

Steven G. Anderson, C. M. Aldao, G. D. Waddill, I. M. Vitomirov,  
S. J. Severtson, and J. H. Weaver

*Department of Chemical Engineering and Materials Science, University of Minnesota, Minneapolis, Minnesota 55455*

(Received 9 June 1989)

Synchrotron-radiation photoemission studies of the formation of Al/GaAs(110) interfaces have been performed as a function of substrate temperature for  $60 \leq T \leq 300$  K for *n*- and *p*-type doped samples. The results show temperature-dependent changes in surface Fermi-level position, surface morphology, and the distribution of released substrate atoms in the overlayer. Detailed examination shows a separation in energy of  $\sim 1.0$  eV for the Al 2*p* binding energy for *n*- and *p*-type GaAs at low coverage. This equals the difference in band bending for the two substrates and demonstrates that the adatom energy reference is an intrinsic level of the semiconductor, not the Fermi level. Substrate band bending approaches its final value when  $E_F$  becomes the energy reference for the overlayer, and this occurs at the onset of metallic overlayer behavior. Temperature-dependent band bending observed below  $\sim 1$  monolayer can be understood in terms of the coupling of an adsorbate energy level to the semiconductor via steady-state tunneling and thermionic emission. The high-coverage results at all temperatures are consistent with metallicity.

### INTRODUCTION

The fundamental physical mechanism(s) and consequences of Schottky-barrier formation have been studied extensively for years. Photoemission has been one of the techniques of choice to study the effects of adatom deposition on semiconductors because of its ability to correlate electrical properties (band bending) with physical and chemical changes at the surface.<sup>1</sup> Of the many metal-GaAs interfaces examined, Al/GaAs has probably received the most attention, in part because Al is a relatively simple metal from a theoretical standpoint (no *d* electrons),<sup>2</sup> because Al-Ga exchange reactions occur at the surface,<sup>1</sup> and because of the importance of Al<sub>*x*</sub>Ga<sub>1-*x*</sub>As/GaAs heterojunctions. Most recently, experiments that emphasized low-temperature Al deposition on GaAs(110) have given new insights into the importance of metallicity in Fermi-level evolution.<sup>3-5</sup>

This paper presents high-resolution synchrotron-radiation photoemission investigations of Al/GaAs(110) interfaces prepared by atom deposition on substrates held at temperatures between 60 and 300 K. The goal was to correlate changes in Al morphology and interface chemistry with Fermi-level movement. The morphology is found to be highly dependent on temperature, while the amount of substrate disruption is not considerably altered by forming an interface at lower temperature. We find that the Al 2*p* core-level position strongly depends on the doping type and extent of band bending at low coverage and temperature, indicating that the energy reference of adsorbed Al atoms is the conduction-band minimum (CBM) or an equivalent intrinsic energy level, not the Fermi level. The low-temperature results show that  $E_F$  ultimately becomes the overlayer energy reference, but only after the deposition of 5–10 Å of Al. At coverages below the metallic limit, the temperature-dependent

band-bending behavior forces a reevaluation of existing Schottky-barrier models and can be understood in terms of the coupling of the adsorbate level with the substrate via steady-state tunneling and thermionic-emission currents. We discuss the results in terms of a recent model of current flow between the bulk and surface of the semiconductor. At higher coverage, the coupling of the overlayer to the bulk semiconductor is enhanced by charge delocalization, i.e., surface metallicity.

### EXPERIMENT

The photoemission experiments were conducted at the University of Wisconsin–Madison Synchrotron Radiation Center, Stoughton, WI, using the Grasshopper Mark II and Mark V monochromators and beamlines. A double-pass cylindrical mirror analyzer mounted in an ultrahigh-vacuum experimental chamber (operating pressure  $\sim 5 \times 10^{-11}$  Torr) was used to acquire photoelectron core-level energy-distribution curves (EDC's).<sup>6</sup> Samples were connected to the second stage of a closed-cycle helium refrigerator via a Cu braid. A resistive heater made it possible to select sample temperatures between 60 and 300 K, as measured with a Si diode (accuracy  $\pm 5$  K). The sample temperature was constant during data acquisition, with no change when the sample was exposed to the Al source.

Clean (110) surfaces were created by cleaving posts of *n*-type (Si doped,  $n = 1 \times 10^{17}$  cm<sup>-3</sup>) and *p*-type (Zn doped,  $p = 2 \times 10^{18}$  cm<sup>-3</sup>) GaAs. Cleave quality was assessed visually and spectroscopically. Surfaces for which  $E_F$  was more than  $\sim 60$  meV from the band edges were rejected. Core-level line-shape decomposition was performed with an IBM PC/RT microcomputer using a nonlinear least-squares curve-fitting program.<sup>7</sup> Aluminum was evaporated from resistively heated W baskets

located  $\sim 35$  cm from the sample. Stable evaporation rates of  $\sim 0.1$  Å/min ( $\sim 1$  Å/min) were set prior to exposure to the Al atom flux for coverages below (above)  $0.5$  Å (pressure  $\leq 2 \times 10^{-10}$  Torr). A quartz crystal microbalance was used to monitor the amount and rate of deposition. Angstroms are used to express the amount of Al deposited. For Al,  $1.47$  Å corresponds to one monolayer (ML) of the GaAs(110) surface, namely  $8.86 \times 10^{14}$  atoms  $\text{cm}^{-2}$ , but layer-by-layer growth is not implied.

## RESULTS AND DISCUSSION

### Surface reactions and Al clustering

Figure 1 shows Ga  $3d$  EDC's for representative depositions at 300 K (left) and 60 K (right). Results for intermediate temperatures fall between these extremes. Line-shape decomposition shows the familiar bulk and surface-shifted components for the clean surface (labeled 1 and 2, respectively) where the latter is shifted  $-0.30$  eV

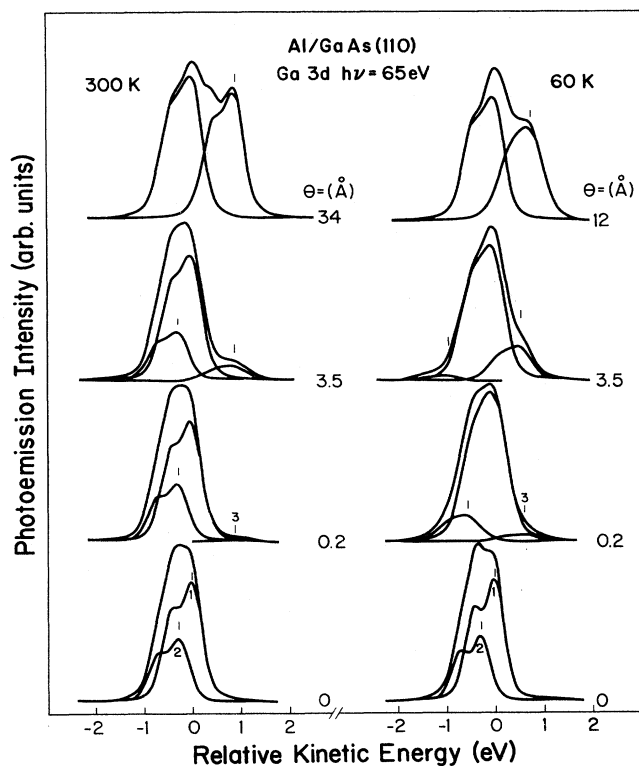


FIG. 1. Ga  $3d$  core-level EDC's for representative Al depositions at 60 and 300 K showing the formation of new Ga features (labeled 3) which grow in relative intensity. The energy position of component 3 shifts gradually to lower binding energy at 60 K but is invariant at 300 K. This reflects differences in Ga coordination in the evolving overlayer. Although different morphologies are observed at 300 and 60 K, there is approximately the same amount of substrate reaction. The gradual shift of the surface-shifted component, labeled 2, at 60 K is likely due to surface unrelaxation and Al—Ga bonding.

and amounts to 34% of the total intensity at  $h\nu = 65$  eV in our collection geometry. The branching ratio is 0.70 compared to the statistical value of 0.67. The clean-surface EDC's measured at 60 K exhibit reduced (Gaussian) broadening compared to those at 300 K, as expected.

As is well known, Al atom mobility on GaAs(110) is relatively high at 300 K, widely separated clusters form spontaneously, and substantial amounts of the surface remain exposed.<sup>8</sup> Hence, the Ga  $3d$  EDC's of Fig. 1 show the persistence of the surface-shifted component until  $\sim 16$  Å. Where Al—GaAs reaction occurs, this surface component disappears and a third component appears at lower binding energy. The large width of this new structure indicates that Ga atoms released from the substrate exist in a variety of chemical environments in the developing overlayer.<sup>9</sup>

The overlayer formed at 60 K is much more uniform than at 300 K because Al surface mobility is orders of magnitude smaller. As a result, the rate of attenuation of the surface component is faster at low temperature (compare Ga EDC's at  $3.5$  Å). Detailed analysis of the 60 K results shows that the surface-shifted component moves to higher binding energy as it decays. This movement is summarized in Fig. 2 where we show the energy spacing between the surface and bulk components as a function of Al deposition at 60 and 300 K. Clearly, the surface-to-bulk energy separation is independent of doping type. This dependence on deposition temperature has not been observed previously. The increasing surface-to-bulk energy spacing cannot be explained in terms of Doniach—Sunjić peak asymmetries because, as will be discussed below, Al does not become metallic until  $\geq 8$  Å deposition (such asymmetry would broaden the EDC's to the left and would complicate analysis).<sup>10</sup> Likewise, it is not due to inhomogeneous band bending because electrostatic effects would broaden the surface and bulk features equally while the spacing between them would be constant.

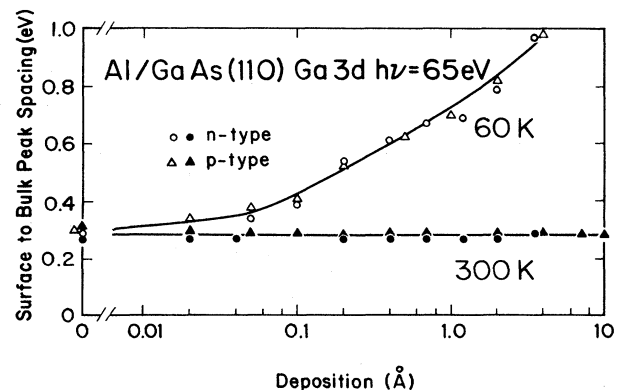


FIG. 2. Energy spacing between surface and bulk Ga  $3d$  core-level energies at 60 K (upward sloping curve) and 300 K (flat line) for *n*- and *p*-type substrates. Atom deposition at 60 K induces a shift of the surface component to larger binding energy, and this trend increases with deposition until the surface is covered at  $\sim 3.5$  Å. Equivalent changes are not observed at 300 K.

We suggest that the shift of the surface feature reflects surface unrelaxation and surface bonding of Al to Ga. The latter has been predicted to occur prior to unrelaxation of the surface.<sup>2,11,12</sup> Unfortunately, the pseudopotential calculations were very sensitive to the bonding geometry, yielding results for the amount of Al-Ga charge transfer that are model dependent. Hence, energy shifts cannot be estimated. The observed increase in surface-to-bulk peak spacing supports the calculations of Priester *et al.* that predicted Ga surface core-level shifts to be 0.58 eV for the unrelaxed surface and 0.38 eV for the relaxed surface.<sup>13</sup> It is likely that some of the observed surface component shift is due to Al-Ga bonding since unrelaxation of the surface alone is not sufficient to explain shifts of up to  $\sim 1$  eV. We note that the calculated surface shifts for As differ by only 0.03 eV for the relaxed and unrelaxed surfaces, and this is also in agreement with the absence of any observable change in our As 3d core levels. Moreover, Zhang *et al.*<sup>2</sup> have shown that Al-Ga wave-function overlap is large for Al on a relaxed GaAs(110) surface, and this may also be consistent with our results. In that case, the total energy of the system would be reduced by  $\sim 0.35$  eV per surface atom, allowing the Al-covered surface to unrelax. This suggests that the increasing peak separation due to unrelaxation and Al-Ga bonding competes with disruption of the substrate via the Al-Ga exchange.

Analysis of the relative intensities for Ga component 3 (Fig. 1) suggests that the amount of released Ga is *greater* for 60 K deposition than for 300 K at low coverages (compare EDC's at 3.5 Å), because differences in overlayer morphology exist. Deposition onto cold substrates produces a more uniform film than for 300 K deposition. Consequently, a greater proportion of the surface is perturbed by adatoms. When the entire surface has been covered, the total amount of substrate disruption is expected to be approximately the same. We note that the position of component 3 relative to the bulk feature is not the same at 60 and 300 K because released Ga atoms are coordinated with Al differently in the two cases. In particular, Ga atoms released by reaction at low temperature are kinetically trapped in the thin Al layer near the interface as will be shown by the attenuation curves of Fig. 3. In contrast, deposition of Al at 300 K results in Ga atoms residing in, and on, the growing Al clusters.<sup>14</sup> The different bonding configurations inferred from the Ga 3d spectra are supported by analysis of the Al 2p core levels which are narrower and more bulklike at 300 K than at 60 K for equivalent depositions.

Figure 3 provides quantitative information about the attenuation of each of the Ga 3d spectral features by plotting  $\ln[I(\theta)/I(0)]$  versus Al deposition, where  $I(0)$  is the total emission from the clean surface and  $I(\theta)$  is the intensity of each component (or the total) after the deposition of  $\theta$  Å of Al. Comparison of the total Ga 3d emission shows much faster reduction at 60 K than at 300 K because cluster formation at 300 K does not effectively cover the surface. For 300 K deposition, emission from the surface component is still evident at 10–15 Å at the  $\sim 5\%$  level, indicating that the clusters have covered most of the surface, but that some areas remain exposed.

In contrast, the surface-shifted component is quenched by  $\sim 3.5$  Å at 60 K with a  $1/e$  length of  $\sim 1.4$  Å. The signal from the disrupted feature increases until 3.5 Å with deposition at 60 K, and is then attenuated less quickly than the bulk component (compare  $1/e$  lengths of 4.5 and 3.2 Å, respectively). The larger attenuation length exhibited by the disrupted component reflects the dissolution of Ga in the overlayer. In contrast, the corresponding reaction-induced feature at 300 K exhibits a plateau at high coverage. These results suggest that Ga atoms released from the substrate are kinetically trapped near the interface at 60 K but segregate to the surface more readily at 300 K. While differences in morphology for 300 and 60 K deposition make quantitative comparisons difficult, the maximum emission from the released component is approximately the same for both temperatures, suggesting that the total amount of substrate disruption is similar.

Several groups have assumed that low temperature Al/GaAs interface formation is accompanied by the inhibition of reaction and defect formation compared to 300 K deposition.<sup>3–5</sup> The results of Fig. 3 indicate that disruption is not quenched and that the amount of reaction is not affected significantly when depositions are made at

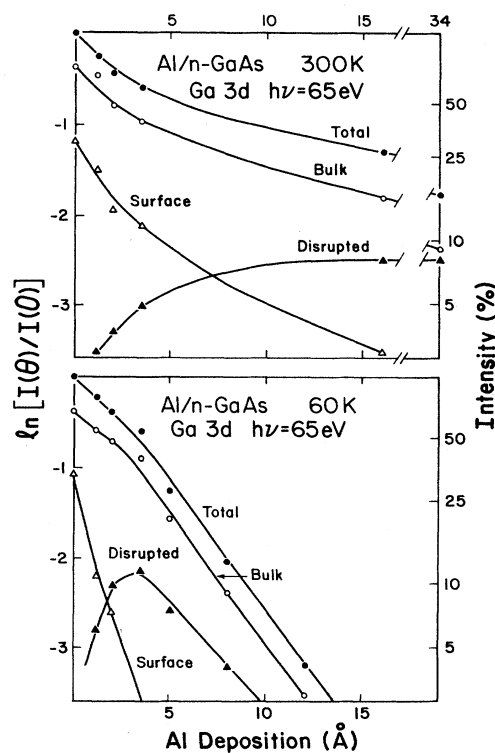


FIG. 3. Attenuation curves for the Ga 3d core-level intensities as a function of Al deposition at 300 and 60 K. Reduced adatom surface mobility at low temperature inhibits three-dimensional cluster formation, thereby leading to more uniform coverage and faster substrate attenuation. Ga atoms released by Al-substrate interaction are kinetically trapped near the interface at 60 K but they can segregate at 300 K.

60 K. Recent studies by Aldao *et al.*<sup>15</sup> for Ti/GaAs(110) and Waddill *et al.*<sup>16</sup> for Co/GaAs(110) have demonstrated rather unambiguously that equivalent surface disruption occurs for atom deposition at 60 and 300 K. We conclude that thermal effects do not eliminate chemical processes and the release of substrate atoms. At the same time, however, temperature does modify the redistribution of released Ga and As atoms. Because diffusion is a thermally activated process, kinetic trapping of the disrupted substrate atoms near the interface is expected to occur at low temperature.<sup>15,16</sup>

The onset of metallicity has attracted considerable attention because wave-function delocalization at the surface facilitates band-bending changes. To investigate this effect, we have studied the Al 2*p* core-level development on *n*- and *p*-type GaAs(110) at 60 K. Representative EDC's are shown in Fig. 4 for coverages above 0.2 Å. Band-bending effects, which were removed from the Ga data in Fig. 1, have not been subtracted here to emphasize that the adatom energy reference changes with

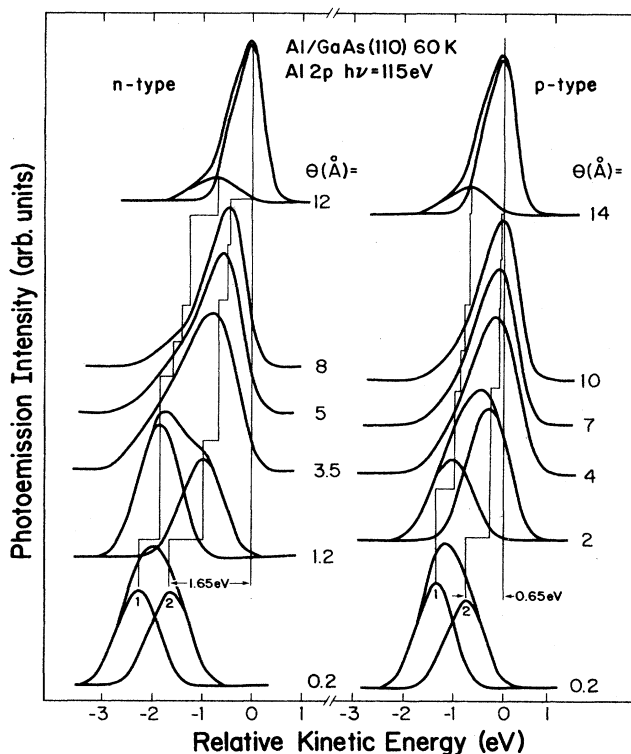


FIG. 4. Al 2*p* core level EDC's as a function of  $\theta$  for deposition onto *n*- and *p*-type GaAs(110) at 60 K. The two components (corresponding to Al atoms interacting with the substrate and Al atoms forming Al clusters) shift to higher kinetic energy with overlayer development, ultimately stabilizing when the overlayer is metallic. For both *n*- and *p*-type GaAs, the energy zero is referenced to  $E_F$  for metallic Al. The different amounts of energy offset indicate that an intrinsic level of the semiconductor is the appropriate reference in the regime when  $E_F$  is changing with band bending.

coverage. Two components are necessary to fit the spectra, even at low coverage, but we find no compelling reason to add a third as proposed in Refs. 4 and 17 to distinguish between isolated adsorbed Al atoms, Al-substrate interactions, and unreacted Al which evolves to the metal. Feature 1 corresponds to Al atoms which have interacted with the substrate while peak 2 is due to unreacted Al in configurations which evolve into metal.<sup>1</sup> Spin-orbit split doublets composed of Voigt functions were used to model the overlayer spectra.<sup>18</sup> As a first approximation, we constrained the spin-orbit splitting, branching ratio, and Lorentzian widths to values measured for thick Al films.<sup>19</sup> The observed core-level features are quite broad [ $\sim 1$  eV full width at half maximum (FWHM)] below  $\sim 4$  Å deposition because dispersed Al atoms exist in a variety of slightly inequivalent bonding configurations. For coverages between 4 and 12 Å, the FWHM narrows to its bulk value of 0.4 eV. (This contrasts with measurements made at 300 K, where the FWHM of 0.5 eV below 4 Å deposition indicates greater tendency to form clusters than the corresponding coverages at 60 K.) Both reacted and unreacted Al atom contributions are present at 0.2 Å. With increasing deposition, the overall structure shifts to lower binding energy and is dominated by a component that corresponds to bulklike Al. For the metallic component, a Doniach-Šunjić line-shape asymmetry is necessary to account for core-hole screening at high coverage.<sup>19</sup>

#### Energy references

Perhaps the most striking aspect of the Al 2*p* core-level EDC's of Fig. 4 is that feature 2 for 0.2 Å Al on *n*-type GaAs is shifted 1.65 eV to higher binding energy relative to the energy of the equivalent peak at highest deposition, as noted, while the corresponding shift for *p*-type GaAs is only 0.65 eV. Significantly, the Al 2*p* features appear at higher binding energy for *n*-type GaAs than for *p*-type GaAs at all coverages below 10 Å, and the difference is approximately the separation in core-level energies for *n*- and *p*-type GaAs substrates below 1 Å (discussed further below). Adsorbate core-level positions have generally been referenced to either the vacuum level or the substrate Fermi level. The vacuum level is difficult to use because the adsorbate core-level position relative to the substrate Fermi level will depend on the work function of the substrate. Since the adsorbate perturbs the substrate work function, considerable confusion generally results unless the surface work function is monitored.<sup>20-22</sup> Use of the substrate Fermi level as the adatom energy reference is not possible in this case because the results of Fig. 4 would imply that the binding energy of isolated Al atoms differs by  $\sim 1$  eV on virtually identical surfaces. This is physically unreasonable and demonstrates that the adatom bonding levels are tied to the substrate at low coverage. Hence, the distinct evolution of the Al 2*p* core-level energy positions exhibited on *n*- and *p*-type GaAs is a consequence of surface electrostatics (band bending).

If the energy levels of adsorbed Al atoms or Al clusters are referenced to the semiconductor CBM, then the pho-

photoelectron kinetic energies can be determined from Fig. 5.<sup>20,21</sup> In the center, we show the relevant energies for the electron energy analyzer in contact with the *n*- or *p*-type semiconductor. The dashed line corresponds to the common Fermi level, and band bending is as sketched. In general, the photoelectron kinetic energy is given by

$$E_k = h\nu - E_B - \varphi_a, \quad (1)$$

where  $h\nu$  is the photon energy,  $E_B$  is the binding energy referenced to  $E_F$ , and  $\varphi_a$  is the analyzer work function. Energy levels can be referenced to the CBM of the *n*- or *p*-type semiconductor rather than  $E_F$  by

$$E_B = E_a - (E_c - E_F), \quad (2)$$

where  $E_a$  is the energy spacing between the core level and the CBM and  $E_c - E_F$  is the difference between the CBM and the Fermi level. The measured kinetic energy of photoelectrons from adsorbed atoms is then

$$E_k = h\nu - E_a + (E_c - E_F) - \varphi_a. \quad (3)$$

Equation (3) allows adatoms on *n*- or *p*-type semiconductors to have the same  $E_a$  with different apparent binding energies, as observed.

When Al is deposited onto GaAs(110), there are Al 2*p* core-level shifts that result from Al-Al interaction (the evolution from isolated atoms to clusters and ultimately metallic Al) and from changes due to Fermi-level movement in the band gap (band bending and Schottky barrier formation). The convergence to bulklike bonding will, in general, shift the core-level emission to higher kinetic energy. The effects of band bending will depend on the doping type. Consideration of band bending in Fig. 5 yields the kinetic energy difference measured for the same adatom or cluster on *p*- and *n*-type samples as

$$E_k^p - E_k^n = (E_c - E_F)_p - (E_c - E_F)_n \cong E_g - \Delta E_p - \Delta E_n. \quad (4)$$

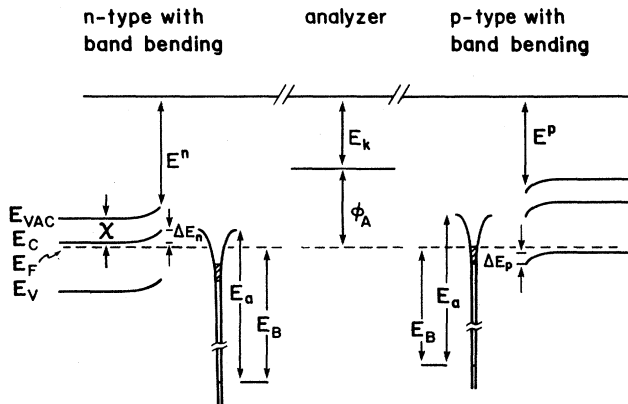


FIG. 5. A schematic of Al adatom or cluster energy  $E_a$  referenced to the CBM of an *n*- and a *p*-type semiconductor with band bending. The offset in kinetic energy for like numbers of adsorbates on the two surfaces will be approximately equal to the band gap minus the sum of the band bending for *n*- and *p*-type surfaces, as observed in Fig. 4.

$\Delta E_p$  and  $\Delta E_n$  represent changes in band bending as directly determined from analysis of the substrate core-level energies. Again, the inexact equality reflects the initial position of  $E_F$  in the gap for clean surfaces. Clearly, band bending reduces the kinetic energy difference for photoelectrons from identical isolated adatoms measured for *n*- and *p*-type semiconductors. Note that Eq. (4) will be valid until the overlayer starts to become metallic, at which point the overlayer energy reference must switch from the intrinsic semiconductor level to  $E_F$ .

Experimentally, adatom deposition induces Fermi-level movement and modification of the overlayer as clusters grow and reaction continues. Surface modifications should be nearly identical for any given coverage for *n*- and *p*-type GaAs, and this is reflected by the line shapes of Fig. 4. (The minor differences at 0.2 Å deposition may be due to slightly inequivalent coverages.) From Eq. (4), the difference in kinetic energies for the Al 2*p* core levels on *n*- and *p*-type substrates should follow the difference in band bending measured from the GaAs core levels as long as their energy reference is an intrinsic level of the semiconductor.

To determine whether these Al/GaAs interfaces do, in fact, evolve equivalently for *n*- and *p*-type GaAs, we mea-

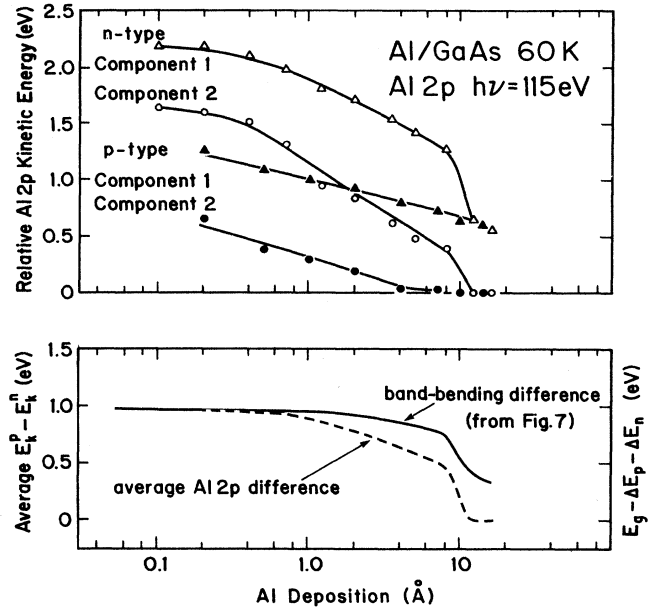


FIG. 6. Top panel: Relative Al 2*p* core-level energies determined from the reacted and cluster components of Fig. 4 (labeled 1 and 2, respectively) as a function of deposition. For the *n*- and *p*-type substrates, they converge to the same energy as the overlayer becomes bulklike and  $E_F$  becomes the energy reference to  $E_F$ . Bottom panel: Average energy separation between the two Al components (from top panel) and the difference in band bending between *n*- and *p*-type GaAs at 60 K. These results show that the energy reference for the overlayer at low coverage is the CBM (or equivalent bulk semiconductor state).  $E_F$  is the reference at high coverage after completion of band bending.

sured the offset between components 1 and 2 of Fig. 4 relative to the metallic Al  $2p$  kinetic energy at high coverage. Again, the energies were determined by line-shape decomposition of the relatively broad Al  $2p$  emission, and the error is estimated to be  $\pm 0.1$  eV. The results are shown in the top panel of Fig. 6. At any coverage below  $\sim 10$  Å, the Al  $2p$  peak positions are shifted to lower kinetic energy for  $n$ -type GaAs relative to  $p$ -type GaAs. The energies for  $p$ -type GaAs increase with deposition, converging to the final position by  $\sim 10$  Å (the zero of Fig. 6). Those for  $n$ -type GaAs also shift but exhibit a step with a midpoint at  $10$  Å. The two components for either type do not run exactly parallel because component 2 is due to unreacted Al (with energy changes related to increasing Al-Al coordination) and component 1 corresponds to reacted Al atoms at the GaAs surface (which evolve because of chemical modification). The coverage-by-coverage separation between like components for  $n$ - and  $p$ -type GaAs should be approximately the same. Of course, both shift during interface evolution because of band bending. As shown, this trend is observed, and we conclude that the interfaces are evolving along equivalent paths.

The difference in relative Al  $2p$  kinetic energies for Al deposition on  $n$ - and  $p$ -type GaAs at  $60$  K is shown in the lower panel of Fig. 6 by a dashed line. This represents the average separation between component 1 on  $n$ - and  $p$ -type substrates and the same average separation for component 2, namely  $E_k^p - E_k^n$  plotted versus deposition. For comparison, the solid line shows the band-bending difference,  $E_g - \Delta E_p - \Delta E_n$ , to be discussed in detail below. The separation in Al  $2p$  peaks is  $\sim 1$  eV at  $0.2$  Å, exhibits a step at  $10$  Å, and is zero by  $\sim 15$  Å. Similar behavior is exhibited by the band-bending-difference curve. The strong correlation in band-bending differences and Al  $2p$  kinetic energy differences shows that Eq. (5) holds below  $\sim 1$  Å. Again, this shows that the adatom energy reference is the CBM (or any intrinsic level of the semiconductor), *not* the Fermi energy. Above  $1$  Å, the separation between the two curves reflects increasing adatom-adatom interaction, and hence better coupling to the substrate. It is important to note that band-bending shifts approach their final value only when the Al energy reference is the substrate Fermi level, and this corresponds to the onset of metallicity.<sup>23</sup> For substrate temperatures above  $60$  K, this occurs at lower coverages, reflecting increased adatom mobility, cluster formation, and earlier adatom wave-function delocalization.

When the CBM is the energy reference for the adsorbed layer, the adatom binding energy can be referenced to the spectrometer Fermi level by taking the measured band bending into account. This has been implicitly adopted in several examinations of the Al/GaAs interface at both low and room temperature.<sup>4,17</sup> It should be done cautiously, however, because simple subtraction of the measured band bending neglects changes in the evolving character of the adatoms. The results shown in the top panel of Fig. 6 demonstrate that the Al  $2p$  binding energies change continuously with deposition, and the difference curves drawn in the bottom panel indicate that these binding energies track with changes in band bend-

ing below  $\sim 10$  Å. This contrasts to the results of Refs. 4 and 17, and it suggests that binding energy shifts reported between “atomic” and “cluster” coverage regimes may simply reflect the continuously varying adatom-adatom interaction with deposition.

#### Temperature-dependent Fermi-level movement

In Fig. 7 we summarize the movement of  $E_F$  during Al atom deposition for substrate temperatures from  $60$  to  $300$  K. Results for atom deposition at  $60$  and  $300$  K were obtained for both  $n$ - and  $p$ -type samples, as shown. Because the energy gap is changing with temperature, we reference the  $n$ -type data to the CBM on the left axis and  $p$ -type data to the valence-band minimum (VBM) on the right axis. Atom deposition at  $100$ ,  $150$ , and  $200$  K onto  $n$ -type GaAs produced band-bending changes intermediate between those obtained at  $60$  and  $300$  K. The values plotted were obtained by averaging shifts observed for surface and bulk sensitive spectra (kinetic energies of  $\sim 40$  and  $\sim 15$  eV, respectively) for Ga  $3d$  and As  $3d$  core levels.

The band-bending behavior of atoms adsorbed on  $p$ -type GaAs at  $60$  and  $300$  K is qualitatively similar to that observed by Stiles *et al.*,<sup>3</sup> Kelly *et al.*,<sup>4</sup> and Cao *et al.*,<sup>5</sup> although no overshoot of the  $E_F$  position is observed at low coverage. At  $300$  K,  $E_F$  lies above the  $60$  K results for coverages above  $0.1$  Å and gradually shifts to  $0.48$  eV above the VBM. Measurements at  $60$  K indicate that initial band bending occurs which places the Fermi level  $0.36$  eV from the VBM for  $\theta = 0.02$  Å. The Fermi level does not change appreciably until  $2$  Å coverage when it rises to  $0.46$  eV above the VBM. Both  $60$  and  $300$  K results show that  $E_F$  eventually moves to  $\sim 0.47$  eV above

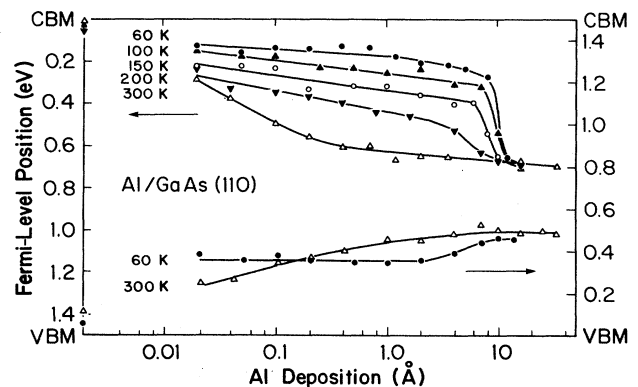


FIG. 7. Fermi-level energy movement as a function of Al coverage and substrate temperature. The left axis is used for the  $n$ -type GaAs results and the right axis for  $p$ -type GaAs to simplify comparison of barrier heights at different temperatures. The movement of the step indicates earlier metallicity for higher temperature because of enhanced surface mobility. The shift of  $E_F$  into the gap as  $T$  increases for a fixed coverage on  $n$ -type GaAs indicates the temperature-dependent coupling of surface and bulk.

the VBM when the metal coverage is sufficiently large, in agreement with Refs. 3–5. The discrepancies between these results and those of others at low coverage can be largely resolved by noting that  $E_F$  movement is quite temperature dependent, as indicated by the  $n$ -type data. Furthermore, the recent results of Aldao *et al.*<sup>23</sup> (discussed below) have shown that the sample doping concentration also affects the amount of band bending produced at low temperature and low coverage.

The results of Fig. 7 show that 0.02 Å of Al on  $n$ -type GaAs at 60 K induces band bending of 120 meV relative to the initial position at 60 K, and  $E_F$  moves rapidly to its final position above 8 Å (midstep at 10 Å). This abrupt change in band bending has been correlated with the onset of metallicity in the overlayer.<sup>24</sup> With increasing temperature, the amount of band bending for a given coverage increases until the final 300 K position is reached, namely 0.70 eV below the CBM. Also, for higher temperature, the step associated with metallicity appears earlier. At 300 K, no inflection in  $E_F$  movement is observed. While these band-bending results are correlated with the onset of metallicity in the overlayer at high coverage, the  $n$ - and  $p$ -type GaAs results do not converge to a common value. We suggest that the coupling between the overlayer and the substrate is not complete within the coverage range that can be investigated with photoemission.<sup>23</sup>

Examination of the Al  $2p$  core-level line shapes and energies (discussed above) showed that the FWHM of unreacted Al narrows substantially over the coverage regime where rapid  $E_F$  movement occurs. In particular, narrowing occurs at lower coverage for higher temperature, in agreement with the coverage and temperature dependence of the Fermi-level step in Fig. 7. These changes in Al emission and the temperature-dependent shifts of the band-bending step can be understood in terms of Al atom surface mobility on GaAs(110). In particular, the onset of metallicity associated with cluster formation is a function of thermally activated surface mobility.<sup>25</sup>

The fascinating low-coverage, low-temperature band-bending behavior exhibited by  $n$ -type GaAs cannot be understood in terms of a metallic overlayer. In particular, by assuming an activation energy of 0.3 eV for Al surface diffusion on GaAs,<sup>25</sup> it can be shown that surface diffusion is negligible below  $\sim 200$  K. Adatoms that are deposited onto cold GaAs surfaces will not readily agglomerate into metallic clusters, and the overlayer morphology will be approximately the same, regardless of temperature. Submonolayer deposition then produces isolated adatoms which induce distinct amounts of band bending at different temperatures, as shown in Fig. 7.

The band bending produced for submonolayer deposition on  $n$ -type GaAs is not consistent with defect models which consider the defects to have discrete energies.<sup>26,27</sup> Adatom deposition will induce  $E_F$  movement only if the adatom-induced states can accept or donate charge. By considering these states to have discrete energies in the band gap, calculations have shown that only  $\sim 10^{12}$  defects/cm<sup>2</sup> are necessary to pin  $E_F$  at the defect energy.<sup>26</sup>

Several conclusions about the relevance of this approach to understanding the results of Fig. 7 can be made. By 0.2 Å of deposition, more than  $10^{14}$  states/cm<sup>2</sup> have been added to the surface. Since adatom deposition induces band bending, these states must lie in the band gap and be able to accept charge ( $n$ -type GaAs). However, the adatom-induced states cannot be fully charged or they would pin  $E_F$  at the defect energy, and no temperature dependence would be observed. Were these defects assumed to have a constant partial charge, the number of them necessary to induce band bending would be greater, but  $E_F$  pinning should be completed within one decade of coverage according to Zur *et al.*<sup>26</sup> and Tang *et al.*<sup>27</sup> This is not observed in Fig. 7 where  $E_F$  movement is induced at the lowest coverage but does not converge to the common final position over more than two decades of Al deposition. This suggests that the average amount of charge on an adatom-induced level is *not* constant with increasing coverage.

The temperature-dependent submonolayer results presented in Fig. 7 cannot be explained in terms of static systems in which adatom-induced states in the gap possess a constant amount of charge. However, we have recently proposed a charge exchange model which considers dynamic exchange between the states at the surface and those in the bulk semiconductor.<sup>23,28</sup> Ultralow deposition produces states at the surface. The net transfer of small amounts of charge to these levels induces band bending with the formation of a depletion region. This is reflected by the gradual band bending exhibited by each of the  $n$ -type GaAs curves below 200 K and 2 Å. Only at higher coverage does the onset of metallic behavior alter the detailed charge balance established in the submonolayer regime.

A simple model of steady-state charge transfer from the bulk to the surface has been developed which successfully describes the experimental results. In particular, the equilibrium current flowing through the junction can be determined by considering tunneling through and emission over the barrier. Since the net current must be zero in equilibrium, the surface-to-bulk current must match the bulk-to-surface current. Our model assumes that each of these currents is constant for a given coverage, independent of sample temperature. For GaAs, tunneling through the barrier established by band bending is the dominant current mechanism below 300 K for  $N = 10^{17}$  cm<sup>-3</sup>.

The tunneling current across the evolving barrier depends on the charge carriers (their number and energy distribution in the conduction band) and on the barrier height and barrier width (which are related by the doping concentration). We postulate that there is a minimal current needed to establish band bending, and that current plays the dominant role in controlling band bending at low temperature for highly doped GaAs. Between 60 and 300 K, increasing the sample temperature does not significantly change the number of electrons in the conduction band for  $n$ -type GaAs, but the average electron energy is increased. This facilitates tunneling and leads to an increase in the steady-state current. Therefore, the current necessary to maintain band bending at

higher temperature can be sustained over a wider depletion region and higher barrier height. However, to keep the equilibrium current constant, the barrier height and depletion width increases. Increased band bending thus counteracts the effect of raising the temperature. Detailed analysis of the model shows a nearly linear dependence of the barrier height on  $T$  for constant coverage in the submonolayer regime. Confirmation of this can be seen directly by inspection of Fig. 7.

### CONCLUSIONS

This paper has shown that the surface morphology for Al/GaAs(110) is temperature dependent, but that the chemistry exhibited at low temperature and room temperature is nearly the same. Adatoms deposited at low temperature unrelax the surface, as shown by detailed line-shape analysis, and the Ga surface core-level shifts are consistent with surface unrelaxation and Al—Ga bonding. Detailed investigation of the overlayer core-level spectra have shown that the proper energy reference

for isolated adatoms is a bulk energy level of the solid, not  $E_F$ . Examination of  $E_F$  evolution as a function of substrate temperatures shows changes which necessitate a reevaluation of defect models. They are in agreement with our charge-exchange model which emphasizes the dynamics of charge exchange between the adatoms at the surface and the substrate beyond the depletion region.

### ACKNOWLEDGMENTS

This work was supported by the U.S. Office of Naval Research under Grants ONR-N00014-87-K-0029 and ONR-N00014-86-K-0427. Core-level spectra were analyzed with IBM PC/RT computers, generously provided through an IBM Materials Science and Processing Grant. Stimulating discussions with B. M. Trafas are appreciated. The photoemission experiments were done at the Wisconsin—Madison Synchrotron Radiation Center, at Stoughton, WI, a user facility supported by the National Science Foundation; the assistance of the staff of that laboratory is gratefully acknowledged.

- <sup>1</sup>See, for example, L. J. Brillson, *Surf. Sci. Rep.* **2**, 123 (1983); J. H. Weaver, in *Analytical Techniques for Thin Films*, Vol. 27 of *Treatise on Materials Science and Technology*, edited by K. N. Tu and R. Rosenberg (Academic, New York, 1988); W. E. Spicer, T. Kendelewicz, N. Newman, K. K. Chin, and I. Lindau, *Surf. Sci.* **168**, 240 (1986); R. Ludeke, *ibid.* **168**, 290 (1986), and extensive references therein.
- <sup>2</sup>S. B. Zhang, M. L. Cohen, and S. G. Louie, *Phys. Rev. B* **34**, 768 (1986). The references cited in this paper provide an overview of theoretical progress made in understanding Al/GaAs interfaces.
- <sup>3</sup>K. Stiles, A. Kahn, D. G. Kilday, and G. Margaritondo, *J. Vac. Sci. Technol. B* **5**, 987 (1987); C. R. Bonapace, D. W. Tu, K. Li, and A. Kahn, *ibid.* **3**, 1099 (1985); C. R. Bonapace, K. Li, and A. Kahn, *J. Phys. (Paris) Colloq.* **45**, C5 (1984).
- <sup>4</sup>M. K. Kelly, A. Kahn, N. Tache, E. Colavita, and G. Margaritondo, *Solid State Commun.* **58**, 429 (1986); M. K. Kelly, N. Tache, G. Margaritondo, and A. Kahn, *J. Vac. Sci. Technol. A* **4**, 882 (1986).
- <sup>5</sup>R. Cao, K. Miyano, T. Kendelewicz, K. K. Chin, I. Lindau, and W. E. Spicer, *J. Vac. Sci. Technol. B* **5**, 998 (1987); M. D. Williams, K. K. Chin, C. E. McCants, P. H. Mahowald, and W. E. Spicer, *ibid.* **4**, 939 (1986); T. Kendelewicz, M. D. Williams, K. K. Chin, C. E. McCants, R. S. List, I. Lindau, and W. E. Spicer, *Appl. Phys. Lett.* **48**, 919 (1986).
- <sup>6</sup>C. M. Aldao, I. M. Vitomirov, F. Xu, and J. H. Weaver, *Phys. Rev. B* **37**, 6019 (1988).
- <sup>7</sup>J. J. Joyce, M. del Giudice, and J. H. Weaver, *J. Electron Spectrosc. Relat. Phenom.* **49**, 31 (1989).
- <sup>8</sup>A. Kahn, *J. Vac. Sci. Technol. A* **1**, 684 (1983), and references therein.
- <sup>9</sup>G. Margaritondo and A. Franciosi, *Annu. Rev. Mater. Sci.* **14**, 67 (1984).
- <sup>10</sup>S. Doniach and S. Šunjić, *J. Phys. C* **3**, 285 (1970).
- <sup>11</sup>J. R. Chelikowski, D. J. Chadi, and M. L. Cohen, *Phys. Rev. B* **23**, 4013 (1981).
- <sup>12</sup>A. Zunger, *Phys. Rev. B* **24**, 4372 (1981).
- <sup>13</sup>C. Priester, G. Allan, and M. Lannoo, *Phys. Rev. Lett.* **58**, 1989 (1987).
- <sup>14</sup>N. G. Stoffel, M. Kelly, and G. Margaritondo, *Phys. Rev. B* **27**, 6561 (1983).
- <sup>15</sup>C. M. Aldao, G. D. Waddill, S. G. Anderson, and J. H. Weaver, *Phys. Rev. B* **40**, 2932 (1989).
- <sup>16</sup>G. D. Waddill, C. M. Aldao, I. M. Vitomirov, S. G. Anderson, C. Capasso, and J. H. Weaver, *J. Vac. Sci. Technol. B* **7**, 950 (1989).
- <sup>17</sup>R. R. Daniels, A. D. Katnani, T.-X. Zhao, G. Margaritondo, and A. Zunger, *Phys. Rev. Lett.* **49**, 895 (1982).
- <sup>18</sup>K. Schönhammer and O. Gunnarsson, *Solid State Commun.* **23**, 691 (1977); J. C. Fuggle, E. Umbach, D. Menzel, K. Wandelt, and C. R. Brundle, *ibid.* **27**, 65 (1978). These studies have shown that the line shape for adsorbates on surfaces may not be completely described by the convolution of Gaussian and Lorentzian functions.
- <sup>19</sup>P. H. Citrin, G. K. Wertheim, and Y. Baer, *Phys. Rev. B* **16**, 4256 (1977).
- <sup>20</sup>P. H. Citrin and G. K. Wertheim, *Phys. Rev. B* **27**, 3176 (1983).
- <sup>21</sup>S. L. Qui, X. Pan, M. Strongin, and P. H. Citrin, *Phys. Rev. B* **36**, 1292 (1987).
- <sup>22</sup>K. Wandelt, in *Thin Metal Films and Gas Chemisorption*, Vol. 32 of *Studies of Surface Science and Catalysis*, edited by P. Wissman (Elsevier, New York, 1987).
- <sup>23</sup>C. M. Aldao, S. G. Anderson, C. Capasso, G. D. Waddill, I. M. Vitomirov, and J. H. Weaver, *Phys. Rev. B* **39**, 12977 (1989).
- <sup>24</sup>K. Stiles and A. Kahn, *Phys. Rev. Lett.* **60**, 440 (1988).
- <sup>25</sup>J. Ihm and J. D. Joannopoulos, *Phys. Rev. Lett.* **47**, 679 (1981); *J. Vac. Sci. Technol.* **21**, 340 (1982).
- <sup>26</sup>A. Zur, T. C. McGill, and D. L. Smith, *Phys. Rev. B* **28**, 2060 (1983).
- <sup>27</sup>J. Y.-F. Tang and J. L. Freeouf, *J. Vac. Sci. Technol. B* **2**, 459 (1984).
- <sup>28</sup>S. G. Anderson, C. M. Aldao, G. D. Waddill, I. M. Vitomirov, C. Capasso, and J. H. Weaver (unpublished).